

## Adsorption Effects in Square-Wave Voltammetry of an EC Mechanism

Valentin Mirčeski<sup>a,\*</sup> and Milivoj Lovrić<sup>b</sup>

<sup>a</sup>*Institute of Chemistry, Faculty of Natural Sciences and Mathematics, Cyril and Methodius University, P. O. Box 162, Skopje 91001, Macedonia*

<sup>b</sup>*Center for Marine Research, Ruđer Bošković Institute, P. O. Box 180, HR-10002 Zagreb, Croatia*

Received December 8, 1998; revised May 21, 1999; accepted July 19, 1999

The influence of adsorption of the electroactive species on the square-wave voltammetric responses of two different EC mechanisms is theoretically studied. Theoretical models for the EC electrode mechanism, coupled with adsorption of the reactant but not of the product of the redox reaction and for the surface EC mechanism in which both the reactant and the product are strongly adsorbed, are developed. The reversible and the quasireversible redox reactions of both electrode mechanisms are considered. Relationships between the properties of the SW response and the parameters of both redox reactions and SW excitation signal are analyzed. The theory is compared qualitatively with the SW voltammograms of azobenzene recorded in an acidic medium.

*Key words:* square-wave voltammetry, EC mechanism, surface EC mechanism, azobenzene

### INTRODUCTION

The study of an electrode reaction coupled with an irreversible follow-up homogeneous reaction (EC mechanism) has been the subject of much research effort during the last several decades because it is one of the more common processes encountered in electrode kinetics.<sup>1–13</sup> Examples of this

---

\* Author to whom correspondence should be addressed.

type of mechanism appear in the oxidation of ascorbic acid<sup>14</sup> and aminophenols,<sup>15</sup> and the reduction of azines,<sup>16</sup> azo dyes<sup>17,18</sup> and certain radicals.<sup>19</sup> Since this mechanism is typical of electrode processes in which organic compounds are involved, it is reasonable to presume that the overall electrode process could be additionally complicated by certain adsorption effects of the electroactive species. For these reasons, an EC electrode mechanism, complicated by adsorption phenomena, has been investigated employing diverse electrochemical techniques, such as cyclic voltammetry,<sup>3,6,7,13</sup> chronocoulometry<sup>4,5</sup> and pulse polarography.<sup>11,12</sup> The general reaction scheme of EC mechanism was discussed by Laviron.<sup>13</sup> It was concluded that the chemical reaction can occur either on the electrode surface, or in the solution near the surface, but these two reactions cannot be distinguished by electrochemical measurements alone.

The square-wave voltammetry, as a complex, multistep chronoamperometric method,<sup>20</sup> is particularly appropriate for studying various types of electrode mechanisms coupled with adsorption phenomena.<sup>21-30</sup> It was shown recently that this technique can be successfully employed for characterization and kinetics measurements of the surface redox reactions.<sup>27,29,30</sup> Although the theory of the square-wave voltammetry of a simple EC mechanism is well known,<sup>8</sup> effects of the adsorption of electroactive species on the EC electrode mechanism have not been the subject of theoretical discussion so far.

In this communication, a theory of the square-wave voltammetry of the following electrode mechanisms is developed:



↓



In the first mechanism, the redox reaction is coupled with both the adsorption of the reactant Ox and homogeneous chemical reaction of the Red product. The second reaction represents a surface EC mechanism in which both species of the redox couple are strongly immobilized on the working electrode surface. In both mechanisms, the reduced form of the redox couple decays to the final product P, through a first-order, chemically irreversible reaction.

The aim of the work is to investigate the theoretical relationships between the properties of the response and both kinetics of the investigated electrode mechanisms and parameters of the excitement signal. The work

also tends to emphasize the discrepancies between the simple EC mechanism (III) and the EC mechanisms coupled with adsorption effects.



The theory is tested on benzidine rearrangement of hydrazobenzene.<sup>31</sup> This system was previously used for testing theoretical models of the surface<sup>7,13</sup> as well as simple<sup>1,2,9,10</sup> and adsorption complicated EC mechanisms.<sup>3,5,11-13</sup> Azobenzene and hydrazobenzene are a well known reversible redox couple.<sup>33-35</sup> In an acidic medium, hydrazobenzene undergoes intramolecular, irreversible rearrangement to benzidine, which is electroinactive.<sup>34,35</sup> Both azobenzene and hydrazobenzene,<sup>5,12,13,36,37</sup> and probably benzidine, are strongly adsorbed to the mercury electrode surface.

## EXPERIMENTAL

Azobenzene (»Merck« for synthesis),  $\text{KNO}_3$ ,  $\text{HNO}_3$ , acetonitrile and standard acetate buffer solution (all »Merck«) were used as received. Redistilled water was used. The stock solution of azobenzene was prepared by dissolving in acetonitrile. Extra pure nitrogen was used for purging the electrolyte solutions for ten minutes prior to each measurement. A nitrogen blanket, over the electrolyte solution, was maintained thereafter.

All voltammograms were recorded using an Autolab multimode polarograph (ECO Chemie, Utrecht, Netherlands) which was connected to a personal computer and a Model 303A static mercury drop electrode (SMDE) from Princeton Applied Research. A platinum wire was used as an auxiliary electrode and an Ag/AgCl (3 mol  $\text{dm}^{-3}$  KCl) electrode as reference.

The measurements were carried out at room temperature.

## MATHEMATICAL MODELS

### *EC Mechanism with Reactant Adsorption*

It is presumed, that under the conditions of a low surface coverage, the adsorption of the reactant obeys a linear adsorption isotherm law, and the mass transport occurs *via* a semi-infinite planar diffusion. Thus, the redox mechanism (I) can be represented mathematically with the following system of differential equations:

$$\delta c_{\text{Ox}} / \delta t = D (\delta^2 c_{\text{Ox}} / \delta x^2) \quad (1)$$

$$\delta c_{\text{Red}} / \delta t = D (\delta^2 c_{\text{Red}} / \delta x^2) - k c_{\text{Red}} \quad (2)$$

where  $k$  is the rate constant of a first-order chemical reaction with unit  $\text{s}^{-1}$ . For simplicity, the diffusion coefficients of both species Ox and Red are supposed to be equal. The above differential equations are solved under the following initial and boundary conditions:

$$t = 0, \quad x \geq 0: c_{\text{Ox}} = c_{\text{Ox}}^*, c_{\text{Red}} = 0, \Gamma_{\text{Ox}} = 0 \quad (\text{a})$$

$$t > 0, \quad x \rightarrow \infty: c_{\text{Ox}} \rightarrow c_{\text{Ox}}^*, c_{\text{Red}} \rightarrow 0, \quad (\text{b})$$

$$x = 0: (c_{\text{Ox}})_{x=0} = K\Gamma_{\text{Ox}} \quad (\text{c})$$

$$D(\delta c_{\text{Ox}}/\delta x)_{x=0} = d\Gamma_{\text{Ox}}/dt + i/nFS \quad (\text{d})$$

$$D(\delta c_{\text{Red}}/\delta x)_{x=0} = -i/nFS. \quad (\text{e})$$

Here,  $c_{\text{Ox}}$  and  $c_{\text{Red}}$  are concentrations of Ox and Red species, respectively,  $c_{\text{Ox}}^*$  is the bulk concentration of Ox species,  $\Gamma_{\text{Ox}}$  is the surface concentration of the adsorbed reactant on the electrode surface,  $K$  is the adsorption constant,  $i$  is the current,  $n$  is the number of electrons,  $F$  is the Faraday constant,  $S$  is the electrode surface area and  $x$ ,  $t$  and  $D$  have their usual meanings. In the equilibrium, Nernst's equation is valid:

$$(c_{\text{Ox}})_{x=0} = (c_{\text{Red}})_{x=0} \exp(\phi), \quad (3)$$

where  $\phi$  is the dimensionless relative electrode potential defined as:  $\phi = (nF/RT)(E - E^0)$ , with the usual meanings of the symbols. If the redox reaction is controlled by the charge transfer rate, the following condition is valid at the electrode surface:

$$i/nFS = k_s \exp(-\alpha \phi)[(c_{\text{Ox}})_{x=0} - (c_{\text{Red}})_{x=0} \exp(\phi)] \quad (4)$$

where  $k_s$  is the standard rate constant of the redox reaction and  $\alpha$  is the transfer coefficient. Applying Laplace transformations, the following integral equations, which relate to the concentration at the electrode surface and the fluxes, are obtained:

$$\begin{aligned} (c_{\text{Ox}})_{x=0} &= c_{\text{Ox}}^* - c_{\text{Ox}}^* \cdot e^{(a^2 \cdot t)} \cdot \text{erfc}(a \cdot \sqrt{t}) - \\ &- a \cdot \int_0^t \frac{i}{n \cdot F \cdot S \cdot \sqrt{D}} \cdot e^{a^2 \cdot (t-\tau)} \cdot \text{erfc}(a \cdot \sqrt{t-\tau}) d\tau \end{aligned} \quad (5)$$

$$(c_{\text{Red}})_{x=0} = \int_0^t \frac{i}{n \cdot F \cdot S \cdot \sqrt{D}} \cdot e^{-k \cdot (t-\tau)} \cdot \frac{1}{\sqrt{\pi \cdot (t-\tau)}} d\tau \quad (6)$$

where  $a = K D^{1/2}$ .

If the redox reaction is reversible, a combination of equations (3), (5) and (6) gives a new integral equation:

$$\begin{aligned}
 c_{\text{Ox}}^* - c_{\text{Ox}}^* \cdot e^{(a^2 \cdot t)} \cdot \text{erfc}(a \cdot \sqrt{t}) - a \cdot \int_0^t \frac{i}{n \cdot F \cdot S \cdot \sqrt{D}} \cdot e^{a^2 \cdot (t-\tau)} \cdot \text{erfc}(a \cdot \sqrt{t-\tau}) d\tau = \\
 = e^\phi \cdot \int_0^t \frac{i \cdot e^{-k(t-\tau)}}{n \cdot F \cdot S \cdot \sqrt{D \cdot \pi \cdot (t-\tau)}} d\tau. \tag{7}
 \end{aligned}$$

The solution for a quasireversible redox reaction is obtained with a combination of equations (4), (5) and (6):

$$\begin{aligned}
 \frac{i}{n \cdot F \cdot S} = k_s \cdot e^{-\alpha\phi} \left[ c_{\text{Ox}}^* - c_{\text{Ox}}^* \cdot e^{(a^2 \cdot t)} \cdot \text{erfc}(a \cdot \sqrt{t}) - a \cdot \int_0^t \frac{i}{n \cdot F \cdot S \cdot \sqrt{D}} \cdot e^{a^2 \cdot (t-\tau)} \cdot \text{erfc}(a \cdot \sqrt{t-\tau}) dt - e^\phi \cdot \int_0^t \frac{i \cdot e^{-k(t-\tau)}}{n \cdot F \cdot S \cdot \sqrt{D \cdot \pi \cdot (t-\tau)}} d\tau \right]. \tag{8}
 \end{aligned}$$

Solutions in the conditions of the square-wave voltammetric excitation signal can be obtained by the numerical method of Nicholson and Olmstead.<sup>38</sup> Both the time variable  $t$  and dimensionless current  $\Psi = i (nFSc_{\text{Ox}}^*)^{-1} (Df)^{-1/2}$  are discretized. To each  $t = m d$  where  $d$  is a time increment, a certain  $\Psi_m$  can be ascribed. The numerical solution for a reversible redox reaction reads:

$$\begin{aligned}
 \Psi_m = \frac{1 - e^{\frac{\beta^2 \cdot m}{50}} \cdot \left( \text{erfc} \left( \beta \cdot \sqrt{\frac{m}{50}} \right) \right) - \frac{1}{5 \cdot \sqrt{2}} \cdot \sum_{i=1}^{m-1} \Psi_i \cdot \left[ \frac{2 \cdot S_{m-i+1}}{\sqrt{\pi}} + \frac{\sqrt{50}}{\beta} \cdot R_{m-i+1} \right]}{\frac{1}{5 \cdot \sqrt{2}} \cdot \left( \frac{2 \cdot S_1}{\sqrt{\pi}} + \frac{R_1 \cdot \sqrt{50}}{\beta} \right) + \frac{e^{\phi_m}}{\sqrt{\gamma}} \cdot M_1} \\
 - \frac{\frac{e^{\phi_m}}{\sqrt{\gamma}} \cdot \sum_{i=1}^{m-1} \Psi_i \cdot M_{m-i+1}}{\frac{1}{5 \cdot \sqrt{2}} \cdot \left( \frac{2 \cdot S_1}{\sqrt{\pi}} + \frac{R_1 \cdot \sqrt{50}}{\beta} \right) + \frac{e^{\phi_m}}{\sqrt{\gamma}} \cdot M_1}. \tag{9}
 \end{aligned}$$

where  $\beta = a f^{-1/2}$ ,  $\gamma = k/f$ ,  $S_m = m^{1/2} - (m-1)^{1/2}$ ,  $R_m = \exp(\beta^2 m/50) \text{erfc}[\beta (m/50)^{1/2}] - \exp[\beta^2 (m-1)/50] \text{erfc}[\beta ((m-1)/50)^{1/2}]$  and  $M_m = \text{erf}[\gamma (m/50)] - \text{erf}[\gamma (m-1)/50]$ .  $f$  is the symbol for the frequency of the SW signal.

The solution for the quasireversible redox reaction reads:

$$\psi_m = \frac{\lambda \cdot e^{-\alpha \cdot \phi_m} \left[ 1 - e^{\beta^2 \cdot \frac{m}{50}} \cdot \left( 1 - \operatorname{erf} \left( \beta \cdot \sqrt{\frac{m}{50}} \right) \right) \right]}{1 + \frac{\lambda \cdot e^{-\alpha \cdot \phi_m}}{5 \cdot \sqrt{2}} \cdot \left( \frac{2 \cdot S_1}{\sqrt{\pi}} + \frac{R_1 \cdot \sqrt{50}}{\beta} \right) + e^{(1-\alpha) \cdot \phi_m} \cdot \frac{\lambda}{\sqrt{\gamma}} \cdot M_1}$$

$$\frac{\lambda \cdot e^{-\alpha \cdot \phi_m} \left[ \frac{1}{5 \cdot \sqrt{2}} \cdot \sum_{i=1}^{m-1} \psi_i \cdot \left( \frac{2 \cdot S_{m-i+1}}{\sqrt{\pi}} + \frac{\sqrt{50}}{\beta} \cdot R_{m-i+1} \right) - \frac{e^{\phi_m}}{\sqrt{\gamma}} \cdot \sum_{i=1}^{m-1} \psi_i \cdot M_{m-i+1} \right]}{1 + \frac{\lambda \cdot e^{-\alpha \cdot \phi_m}}{5 \cdot \sqrt{2}} \cdot \left( \frac{2 \cdot S_1}{\sqrt{\pi}} + \frac{R_1 \cdot \sqrt{50}}{\beta} \right) + e^{(1-\alpha) \cdot \phi_m} \cdot \frac{\lambda}{\sqrt{\gamma}} \cdot M_1} \quad (10)$$

where  $\lambda = k_s / (Df)^{1/2}$ . For these calculations, the time increment is  $d = 1/(50f)$ , which means that each SW half-period is divided into 25 increments.

In the case where the reactant does not adsorb to the electrode surface, the electrode mechanism (I) turns to the simple EC mechanism (III). It corresponds to the following condition:  $\lim (\Gamma_{\text{Ox}}) = \lim ((c_{\text{Ox}})_{x=0} / K) = 0$ . Thus, the SW response of the redox mechanism (III) was simulated as a control reaction. It was also compared with the response of reaction (I) in order to elucidate the differences that arise due to the adsorption of reactant Ox. The solution for reaction (III) was found in the literature.<sup>8</sup>

Square-wave potential signal is a train of cathodic and anodic pulses superposed to a staircase potential ramp. The signal is characterized by amplitude  $E_{\text{sw}}$ , which is half of the peak to peak height, the frequency of pulses  $f$  and the scan increment  $dE$ .

### Surface EC Mechanism

Mathematical model for the surface EC mechanism is based on the following assumptions: both the reactant Ox and the product Red, as well as the final product P, are strongly adsorbed to the electrode surface. The adsorption of both electroactive species is a totally irreversible process and no significant desorption occurs during the experiment. The electrode is well below saturation and there are no interactions between the adsorbed particles. The redox reaction proceeds only from the adsorbed state and the volume redox reaction may be neglected. Under these conditions, the electrode mechanism (II) is described mathematically by the following set of differential equations:

$$d\Gamma_P/dt = k\Gamma_{\text{Red}} \quad (11)$$

$$i/(nFS) = -d\Gamma_{\text{Ox}}/dt \quad (12)$$

$$i/(nFS) = d\Gamma_{\text{Red}}/dt + d\Gamma_P/dt \quad (13)$$

$$t = 0: \Gamma_{\text{Ox}} = \Gamma^*, \Gamma_{\text{Red}} = 0, \Gamma_P = 0 \quad (a)$$

$$t > 0: \Gamma_{\text{Ox}} + \Gamma_{\text{Red}} + \Gamma_P = \Gamma^* \quad (b)$$

If the redox reaction is reversible, Nernst's equation is valid:

$$\Gamma_{\text{Ox}} = \Gamma_{\text{Red}} \exp(\phi) \quad (14)$$

where  $\phi = nF/(RT)(E - E^0_{\Gamma_{\text{Ox}}/\Gamma_{\text{Red}}})$ . If the redox reaction is controlled by the rate of the charge transfer, the following condition on the electrode surface is satisfied:

$$i/(nFS) = k_s \exp(-\alpha\phi) [\Gamma_{\text{Ox}} - \exp(\phi)\Gamma_{\text{Red}}] \quad (15)$$

where  $\Gamma_{\text{Ox}}$ ,  $\Gamma_{\text{Red}}$  and  $\Gamma_P$  are surface concentrations of Ox, Red and P species, respectively,  $\Gamma^*$  is the surface concentration of the initially adsorbed reactant.

The above set of differential equations is solved applying Laplace transformations. The numerical solutions were obtained by the previously mentioned method of Nicholson and Olmstead.<sup>38</sup> The solution for a reversible and quasireversible redox reaction reads, respectively:

$$\psi_m = \frac{1 - \frac{1}{50} \cdot \sum_{i=1}^{m-1} \psi_i - \frac{1}{\gamma} \cdot e^{\phi_m} \cdot \sum_{i=1}^{m-1} \psi_i \cdot M_{m-i+1}}{\frac{1}{50} + \frac{1}{\gamma} \cdot e^{\phi_m} \cdot M_1} \quad (16)$$

$$\psi_m = \frac{\omega \cdot e^{-\alpha\phi_m} - \frac{\omega \cdot e^{-\alpha\phi_m}}{50} \cdot \sum_{i=1}^{m-1} \psi_i - \frac{\omega}{\gamma} \cdot e^{(1-\alpha)\phi_m} \cdot \sum_{i=1}^{m-1} \psi_i \cdot M_{m-i+1}}{1 + \frac{\omega \cdot e^{-\alpha\phi_m}}{50} + \frac{\omega}{\gamma} \cdot e^{(1-\alpha)\phi_m} \cdot M_1} \quad (17)$$

where  $\Psi = i(nFS\Gamma^*f)^{-1}$  is dimensionless current,  $\omega = k_s/f$ ,  $\gamma = k/f$  and  $M_m = \exp[-\gamma(m-1)/50] - \exp(-\gamma m/50)$ . All other symbols have the same meaning as in the previous model.

## RESULTS AND DISCUSSION

*EC Mechanism with Reactant Adsorption*

The dimensionless SW voltammograms are current-potential bell-shaped curves characterized by a dimensionless peak current  $\Delta\Psi_p = \Delta i_p (nFSc_{Ox}^*)^{-1} (Df)^{-1/2}$ , peak potential  $E_p$  and half-peak width  $\Delta E_{p/2}$ . The number of points constituting a voltammogram depends on the scan increment  $dE$ . The point with the highest current value defines the peak current, while its position on the potential axis corresponds to the peak potential. The width of the peak at its half height, expressed in Volts, represents the value of the half-peak width.

The dimensionless SW response of a reversible redox reaction defined by equation (9) is mainly controlled by the adsorption argument  $\beta = a/f^{1/2}$  and chemical argument  $\gamma = k/f$ . The adsorption parameter can be also expressed as a function of the real parameters of the system:  $\beta = K(D/f)^{1/2}$ . This parameter includes both the effect of the mass transport of the electroactive species towards the electrode and the strength of its adsorption on the electrode surface. The chemical parameter  $\gamma$  represents the influence of the following chemical reaction rate on the voltammetric response.

The strength of the adsorption depends inversely on the adsorption parameter  $\beta$ . If  $\beta \geq 0.7$ , the adsorption of the reactant is so weak, that it shows no effect on the voltammetric response. Under these conditions, the adsorption complicated EC mechanism (I) turns to the simple EC mechanism (III), and the dimensionless responses of both electrode reactions are equal. However, if the adsorption of the reactant is significant ( $\beta = 7 \times 10^{-4}$ ), appreciable discrepancies appear between the responses of reactions (I) and (III) (see Figure 1). Due to the adsorptive accumulation of the reactant, the net SW response of reaction mechanism (I) is higher than that of reaction (III). However, its peak potential is shifted in negative direction, since higher energy is needed for the redox reaction which proceeds from the adsorbed state of the reactant. The shift of the peak potential is proportional to the strength of the adsorption. Thus, regardless of the rate of the following chemical reaction, a linear relationship was found between the peak potential and the adsorption constant with a constant slope:  $\Delta E_p / \Delta \log(K) = 2.3 RT / (nF)$ .

The influence of the chemical parameter  $\gamma$  on the dimensionless peak current for diverse adsorption constants is presented in Figure 2. Numerical simulations show that, for any adsorption constant, the peak current depends sigmoidally on the logarithm of the chemical parameter  $\gamma$  (curves 1–3). If  $\log(\gamma) \leq -1.8$ , the follow-up chemical reaction exhibits no influence on the peak current. This situation corresponds to the redox mechanism compli-

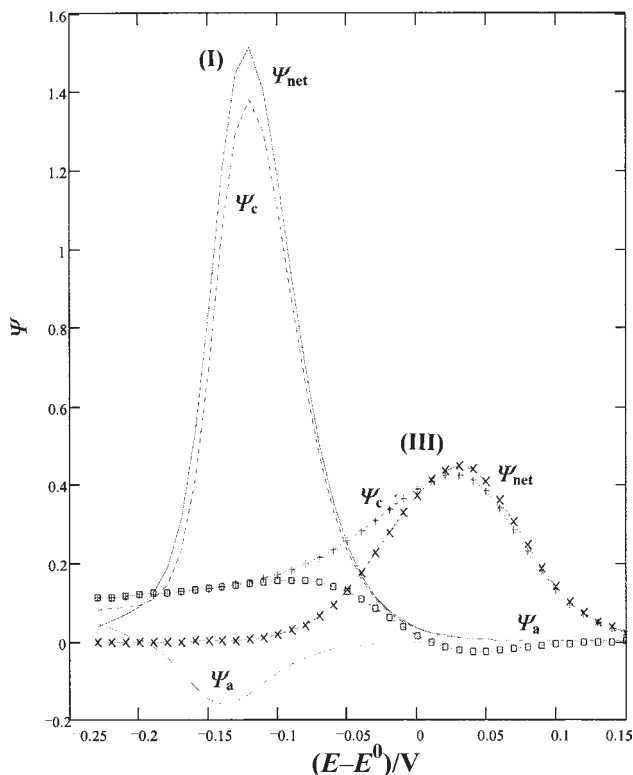


Figure 1. Comparison of the theoretical SW responses of the adsorption complicated EC mechanism (reaction I) and the simple EC mechanism (reaction III). The conditions of the simulations were:  $\log(\gamma) = 0$ ,  $E_{\text{sw}} = 50$  mV,  $dE = 10$  mV (for both reactions) and  $t_{\text{acc.}} = 1$  s and  $\log(\beta) = -3.15$  (for reaction I). Subscripts a, c and net with the symbols for the dimensionless current  $\Psi$  represent the anodic, cathodic and net components of the dimensionless SW response, respectively. Reversible redox reaction.

cated only by adsorption of the reactant. Within the region  $-1.4 \leq \log(\gamma) \leq 0$ , the peak current diminishes proportionally to the increase of  $\log(\gamma)$ . However, the slope of this linear portion depends on the adsorption constant. The stronger the adsorption, the more severe is the influence of the chemical reaction rate on the dimensionless peak current. In the simple EC mechanism (curve 4), the peak current is much less sensitive to the rate of the chemical reaction, as compared to the adsorption complicated EC mechanism.

If  $\log(\gamma) \geq 0.3$ , the peak current becomes independent of the rate of the chemical reaction, which means that the entire amount of the Red species formed as a product of the redox reaction, undergoes immediate chemical

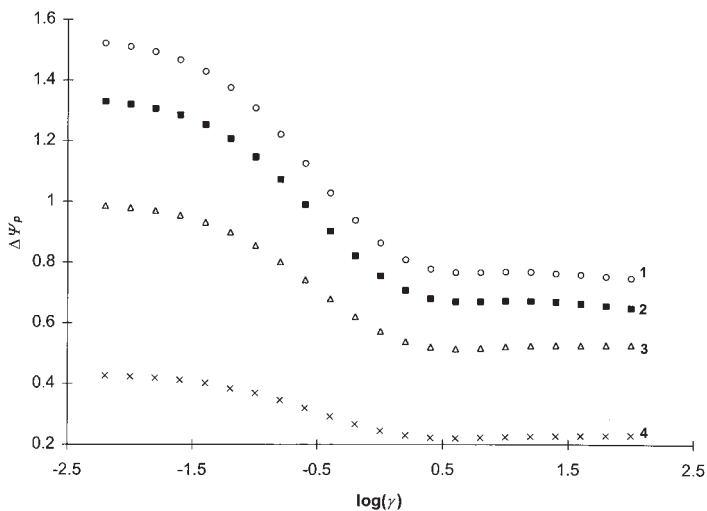


Figure 2. A reversible redox reaction of the adsorption complicated EC mechanism. The effect of the chemical parameter  $\gamma$  on dimensionless peak currents. The conditions of the simulations were:  $E_{sw} = 25$  mV,  $dE = 5$  mV,  $t_{acc.} = 1$  s and  $\log(\beta) = -3.15$  (1);  $-2.15$  (2);  $-1.15$  (3). The curve (4) corresponds to the simple EC mechanism.

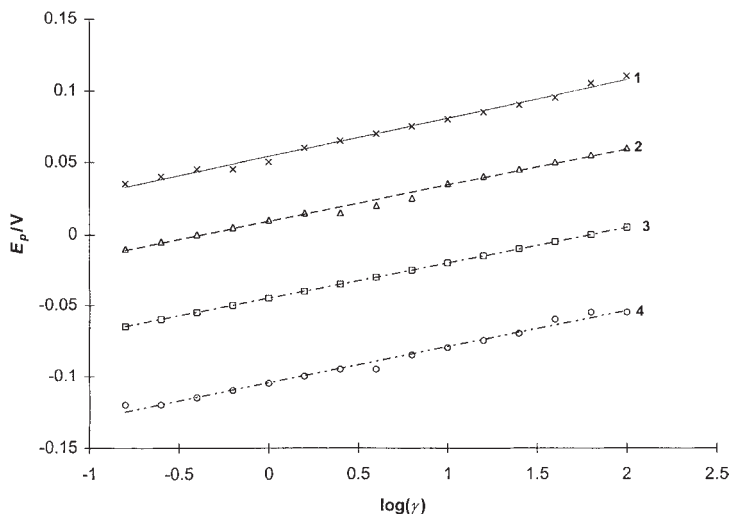


Figure 3. A reversible redox reaction of the adsorption complicated EC mechanism. A relationship between the peak potentials and the logarithm of the chemical parameter  $\gamma$ . All conditions are the same as in the Figure 2. The adsorption parameter is:  $\log(\beta) = -3.15$  (1);  $-2.15$  (2);  $-1.15$  (3). The curve (4) corresponds to the simple EC mechanism.

transformation to the final product P. Therefore, the overall electrode reaction appears totally irreversible.

The dimensionless response  $\Psi$  defined by equation (9) depends on a complex, potential dependent argument  $\exp(\phi)/\gamma^{1/2}$ . It is reasonable to suppose that the SW peak current is associated with a certain critical value of this argument:  $\exp(\phi)/\gamma^{1/2} = p$ . Therefore,  $E_p = E^0 + (1/2)RT/(nF) \ln(\gamma) + (RT/nF) \ln(p)$ . This equation predicts a linear relationship between the peak potential and logarithm of the chemical parameter  $\gamma$ , which was confirmed by the results presented in Figure 3. For any adsorption constant (curves 1–3), linear dependence is observed between the peak potential and logarithm of  $\gamma$ , with a constant slope  $\Delta E_p/\Delta \log(\gamma) = 2.3RT/(2nF)$ . The same dependence exists in the simple EC mechanism (curve 4, Figure 3).

When a particular electrode mechanism is investigated experimentally, the instrumental parameters that can be varied are the frequency of signal  $f$ , the height of the SW pulses  $E_{sw}$  and the scan increment  $dE$ . Variation of the signal frequency has a simultaneous influence on both the adsorption parameter  $\beta$  and the chemical parameter  $\gamma$ . Numerical simulations performed for diverse values of the chemical rate constant  $k$  revealed that the dimensionless peak current depended linearly on the square root of the signal frequency. Keeping in mind that the dimensionless peak current is defined

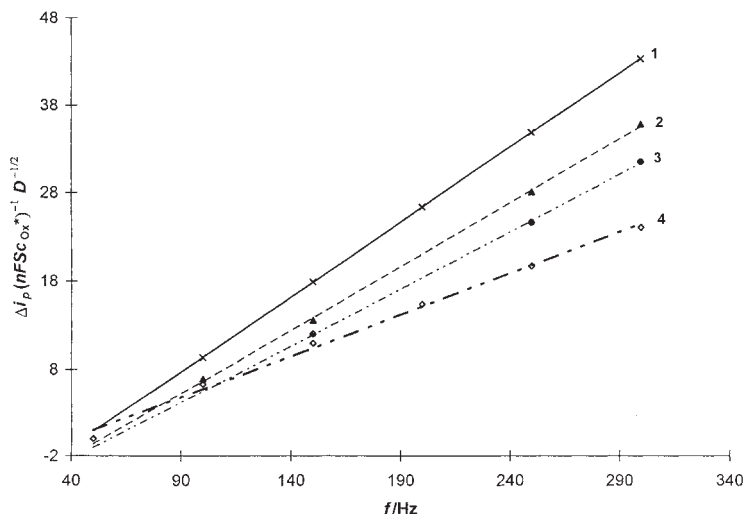


Figure 4. A reversible redox reaction of the adsorption complicated EC mechanism. The dependence of the normalized real peak current on the frequency of the SW signal. The conditions of the simulations were:  $E_{sw} = 20$  mV,  $dE = 5$  mV,  $K = 1$  cm<sup>-1</sup>,  $t_{acc.} = 1$  s. The rate constant of the following chemical reaction is  $k = 10$  (1); 50 (2); 100 (3) and 1000 s<sup>-1</sup> (4).

as  $\Delta\Psi_p = \Delta i_p (nFSc_{Ox}^*)^{-1}(Df)^{-1/2}$ , one can conclude that the real peak current is a linear function of the signal frequency (Figure 4). This is a general property of the reversible redox reaction of all redox processes that proceed from an adsorption state of the reactant.<sup>22, 26</sup> It is worth noting that this is not a property of the simple EC mechanism, where the real peak current is a linear function of the square root of the SW frequency.<sup>8</sup> Being linearly proportional to the logarithm of the frequency, the peak potential shifts in negative direction with an increase in frequency (Figure 5). All the lines presented in Figure 5, have approximately the same slope, however their intercepts are determined by the particular values of the rate constant of the chemical reaction.

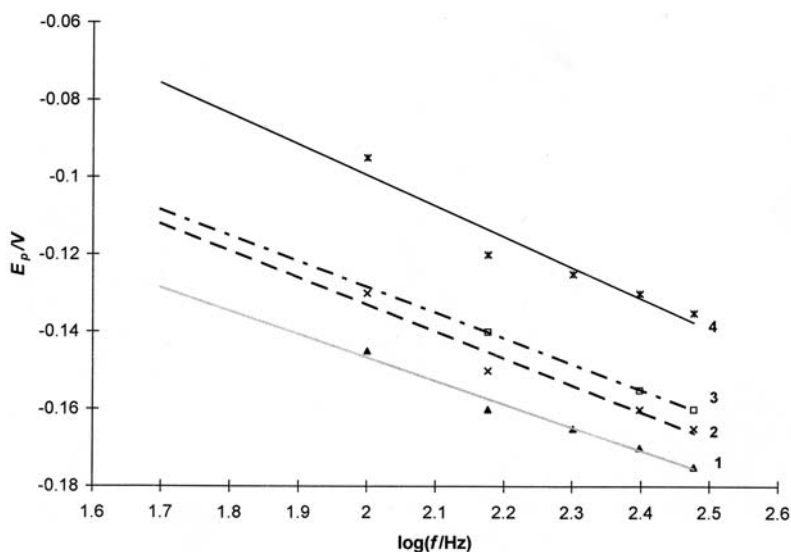


Figure 5. A reversible redox reaction of the adsorption complicated EC mechanism. The dependence of the peak potentials on the logarithm of the frequency of the SW signal. All conditions are the same as in Figure 4. The rate constant of the following chemical reaction is  $k = 10$  (1);  $50$  (2);  $100$  (3) and  $1000 \text{ s}^{-1}$  (4).

The influence of the SW amplitude on both the peak potential and the peak current is presented in Figure 6. The SW peak current increases linearly with the amplitude only within a narrow interval:  $2 \leq E_{sw}/\text{mV} \leq 20$  (Figure 6, curve 1). For larger amplitudes, the linearity is lost and the curve passes through a maximum for  $E_{sw} = 40 \text{ mV}$ . The peak potential becomes more negative proportionally to the increase of the amplitude from 10 to 100 mV (Figure 6, curve 2). The half-peak width is also sensitive to the

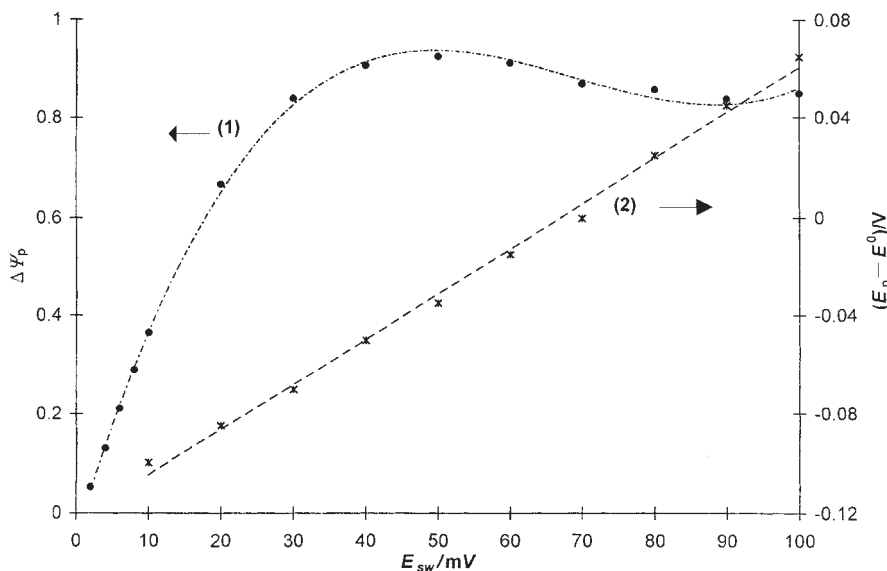


Figure 6. A reversible redox reaction of the adsorption complicated EC mechanism. The influence of the SW amplitude on dimensionless peak currents (curve 1, left axis) and peak potentials (curve 2, right axis). The conditions of the simulations were:  $\log(\gamma) = 1$ ,  $\log(\beta) = -3.15$ ,  $dE = 5$  mV,  $t_{acc.} = 1$  s.

variation of the SW amplitude. The amplitude  $E_{sw} = 50$  mV ensures the highest ratio  $\Delta\Psi_p / \Delta E_{p/2}$ , and hence it is the best value for analytical purposes.

If the redox reaction is partly controlled by the charge transfer rate, in addition to the adsorption parameter  $\beta$  and chemical parameter  $\gamma$ , a new kinetic parameter appears:  $\lambda = k_s / (Df)^{1/2}$  (see equation 10). Parameter  $\lambda$  is defined through the standard rate constant, representing the influence of the charge transfer rate.

The influence of the chemical parameter  $\gamma$  on the dimensionless response of a quasireversible redox reaction is almost the same as in the case of a reversible redox reaction. The dimensionless peak current depends also sigmoidally on the logarithm of  $\gamma$ . The interval  $-1.5 \leq \log(\gamma) \leq 0$  is characterized by a linear dependence between the peak current and logarithm of the chemical parameter, with a slope dependent on both the adsorption parameter  $\beta$  and kinetic parameter  $\lambda$ . The peak potential is insensible to the rate of the chemical reaction if  $\log(\gamma) \leq 0$ . When the redox reaction appears irreversible ( $\log(\gamma) \geq 0$ ), the peak potential is shifted towards more positive values, proportionally to the increase of the logarithm of  $\gamma$ . The slope of this linear relationship is less than  $2.3RT / (2nF)$  which was found for a reversible redox re-

action, and its particular value depends on both the adsorption parameter  $\beta$  and the kinetic parameter  $\lambda$ .

The influence of the kinetic parameter  $\lambda$  on the dimensionless peak current, for various values of  $\gamma$ , is presented in Figure 7. If  $\log(\gamma) = -2$ , the influence of the following chemical reaction can be neglected and, therefore, the

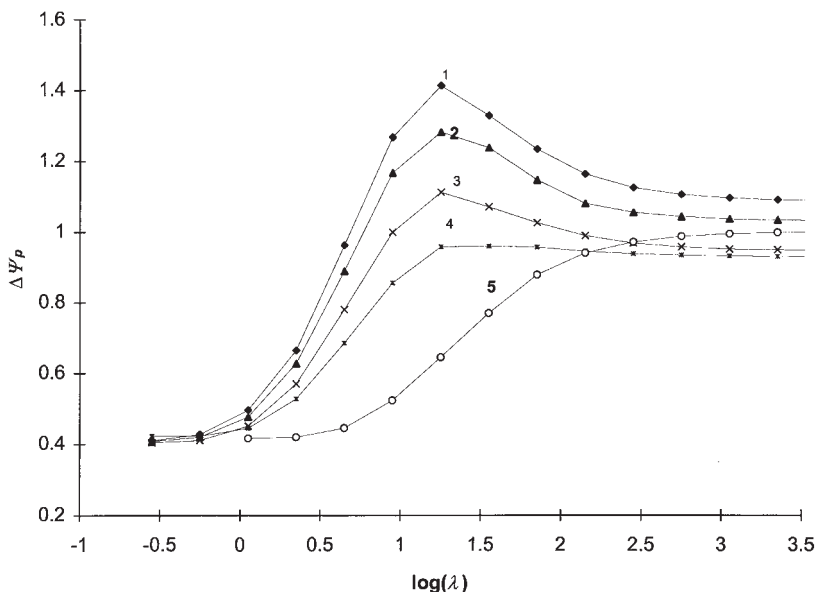


Figure 7. A quasireversible redox reaction of the adsorption complicated EC mechanism. The influence of the kinetic parameter  $\lambda$  on dimensionless peak currents. The conditions of the simulations were:  $E_{sw} = 25$  mV,  $dE = 5$  mV,  $t_{acc.} = 1$  s,  $\alpha = 0.5$ ,  $\log(\beta) = -2.15$ . The chemical parameter is:  $\log(\gamma) = -2$  (1);  $-1$  (2);  $-0.5$  (3);  $0$  (4) and  $2$  (5).

electrode mechanism (I) transforms into the simple redox reaction complicated only by the reactant adsorption (see curve 1 in Figure 7). The adsorption complicated redox reaction is characterized by a nonlinear dependence between the dimensionless peak current and the kinetic parameter  $\lambda$ . Within the interval  $-0.25 \leq \log(\lambda) \leq 1.85$ , the redox reaction appears quasireversible. The quasireversible region is marked by the highest current, and this phenomenon is known as »a quasireversible maximum«. <sup>22,23,25-27</sup> The quasireversible maximum appears as a consequence of the current sampling procedure used in the SW voltammetry. Indeed, when the frequency of the signal was synchronized with the charge transfer rate, the highest current was obtained. The quasireversible maximum appears to be the most important property of

all the electrode processes of immobilized reactant and/or product of the redox reaction. The position of the quasireversible maximum of the adsorption complicated redox reaction depends on the transfer coefficient  $\alpha$  and the pulse height  $E_{sw}$  of the SW excitation signal.<sup>23, 27</sup>

The quasireversible maximum was also observed in the adsorption complicated EC mechanism if the chemical parameter was within the interval  $-2 \leq \log(\gamma) \leq 0$  (curves 2 and 3 in Figure 7). Although the peak currents diminish with an increase of  $\gamma$ , the quasireversible maximum does not depend on this parameter and, hence, its position remains the same as in the case of the simple adsorption complicated redox reaction. This implies that the quasireversible maximum is a property purely determined by the charge transfer rate, and therefore it is solely determined by the kinetic parameter  $\lambda$ . If  $\log(\gamma) \geq 0$ , the rate of the chemical reaction is sufficient to transform all of the Red species into the final product P, immediately after its creation at the electrode surface. Under these conditions, the quasireversible maximum vanishes, and the dimensionless peak current depends sigmoidally on the kinetic parameter  $\lambda$  (Figure 7, curves 4 and 5). The quasireversible maximum was not observed in the simple EC mechanism and therefore this feature can be regarded as the main difference between the quasireversible redox reactions of mechanisms (I) and (III).

### *Surface EC Mechanism*

Generally speaking, the surface EC mechanism behaves in a fairly similar way to the adsorption complicated EC mechanism. Therefore, only some specific properties of this mechanism will be discussed hereafter.

If the redox reaction is reversible, its dimensionless response depends on the chemical parameter  $\gamma$ , according to equation (16). Dependence between the dimensionless peak current  $\Delta\Psi_p$  and the logarithm of  $\gamma$  resembles the corresponding dependence in the adsorption complicated EC mechanism (see Figure 2). The peak potential of the reversible surface EC mechanism is defined as follows:  $E_p = E^0 + RT/(nF) [\ln(\gamma) - \ln(p)]$ , where  $p$  is a certain critical value of the potential dependent argument  $\exp(\phi)/\gamma$  (see Eq. (16)). Therefore, a linear dependence exists between the peak potential and the logarithm of  $\gamma$  with a constant slope:  $\Delta E_p/\Delta \log(\gamma) = 2.3RT/(nF)$ . Note, that the corresponding dependence for the adsorption complicated EC mechanism is characterized by a slope:  $\Delta E_p/\Delta \log(\gamma) = 2.3RT/(2nF)$ .

An increase in the amplitude of the excitation signal exhibits a rather interesting effect on the dimensionless response of the reversible surface EC mechanism. Figure 8 shows that under suitable experimental conditions, the net SW peak is split into two almost symmetrical peaks. The splitting of

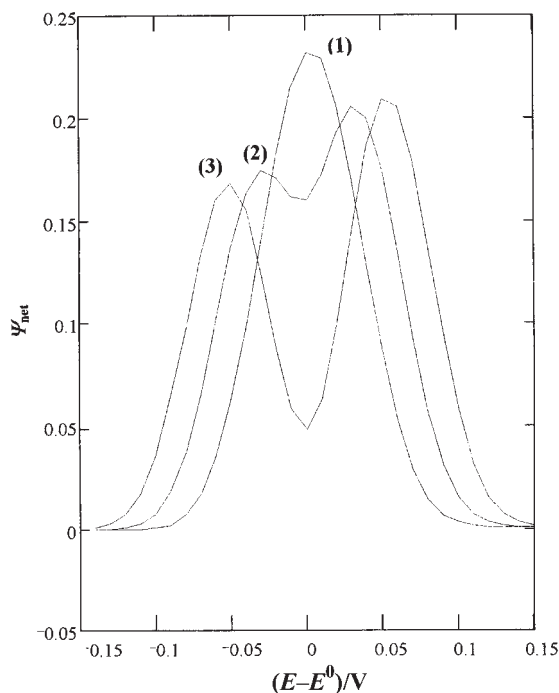


Figure 8. A reversible redox reaction of the surface EC mechanism. Splitting of the SW peak under the influence of the SW amplitude. The conditions of the simulations were:  $\log(\gamma) = -1.5$ ,  $dE = 10$  mV. The SW amplitude is: 30 (1); 50 (2) and 70 mV (3).

the net SW peak arises as a consequence of the enlarged separation between the peak potentials of the cathodic and anodic branches of the SW response.<sup>29</sup> Numerical simulations showed that the separation between the split peaks increased proportionally to the SW amplitude, while it was independent of the chemical parameter  $\gamma$ . On the other hand, the peak current ratio  $\Psi_{p,a}/\Psi_{p,c}$  of the split peaks is highly sensitive to the chemical parameter  $\gamma$  (see inset to Figure 9). The split peaks are equal and symmetrically located around the standard redox potential (see Figure 9, curve 1), only if  $\log(\gamma) \leq -2$ . When the rate of the chemical reaction begins to increase, the anodic peak current gradually diminishes and consequently the ratio  $\Psi_{p,a}/\Psi_{p,c}$  decreases (see inset to Figure 9). If the rate of the chemical reaction is sufficiently rapid to transform all of the Red species into the final product P ( $\log(\gamma) \geq -0.2$ ), the anodic peak vanishes and the splitting of the peak cannot be observed. The splitting of the SW peak is a unique property of the surface EC mechanism. It can be utilized as a simple diagnostic criterion to distinguish this mechanism from either the adsorption complicated (I) or simple EC mechanisms (III).

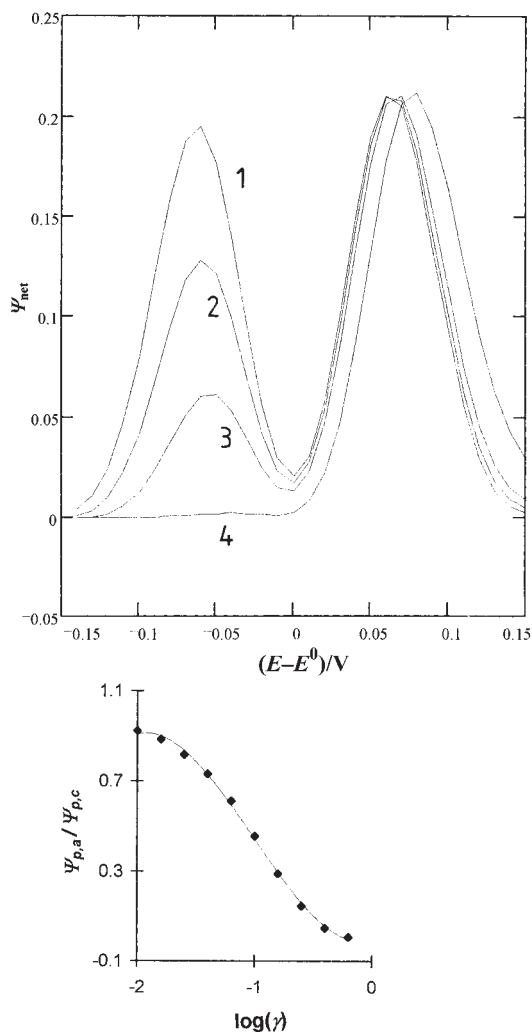


Figure 9. A reversible redox reaction of the surface EC mechanism. The effect of the chemical parameter  $\gamma$  on the splitting of the SW peak.. The conditions of the simulations were:  $E_{sw} = 80$  mV,  $dE = 10$  mV,  $\log(\gamma) = -2$  (1);  $-1.2$  (2);  $-0.8$  (3) and  $-0.2$  (4). The inset shows the dependence of the ratio  $\Psi_{p,a}/\Psi_{p,c}$  on the logarithm of the chemical parameter  $\gamma$ .

If the redox reaction of the surface EC mechanism appears quasireversible, according to Eq. (17), its voltammetric response is controlled by the kinetic parameter  $\omega = k_s/f$  and chemical parameter  $\gamma$ . As can be expected, the dimensionless peak current again depends sigmoidally on the logarithm of  $\gamma$ . However, the linear portion of this dependence has a slope depending on

the kinetic parameter  $\omega$ . The peak potential depends linearly on the logarithm of  $\gamma$  only if  $\log(\gamma) \geq -0.5$ . The slope of this line is dependent on the kinetic parameter  $\omega$  and it is less than the corresponding value found for the reversible redox reaction:  $\Delta E_p / \Delta \log(\gamma) = 2.3RT/(nF)$ .

The dimensionless peak current of the quasireversible surface EC reaction depends almost parabolically on the kinetic parameter  $\omega$ , forming »a quasireversible maximum«. Similarly to the previous model, the position of the quasireversible maximum is entirely determined by the charge transfer rate and it is independent of the chemical parameter  $\gamma$  (see Figure 10). Regardless of the particular value of the chemical parameter  $\gamma$ , the position of

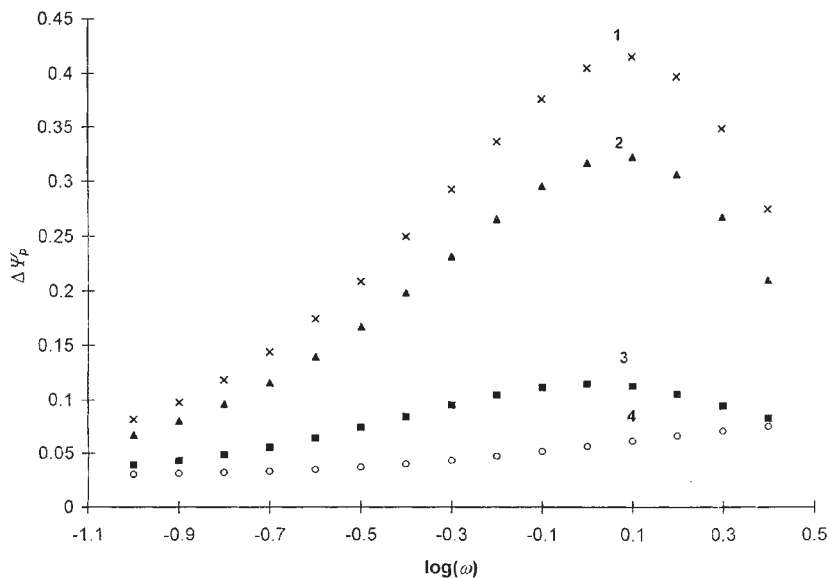


Figure 10. A quasireversible redox reaction of the surface EC mechanism. The effect of the kinetic parameter  $\omega$  on the dimensionless peak currents for different values of the chemical parameter  $\gamma$ . The conditions of the simulations were:  $E_{sw} = 20$  mV,  $dE = 5$  mV,  $\alpha = 0.5$ ,  $\log(\gamma) = -2$  (1);  $-1$  (2);  $0$  (3) and  $1$  (4).

the quasireversible maximum is the same as in the case of the simple surface redox reaction (see curves 1–3 in Figure 10). Like in the previous model, the quasireversible maximum is a property that entirely depends only on the kinetic parameter  $\omega$ . These results are particularly important since they demonstrate that the method recently developed for kinetic measurements of the surface redox reactions, based on the quasireversible maximum,<sup>25–27</sup> can be also applied to the surface EC redox reaction.

## EXPERIMENTAL RESULTS

Theoretical calculations are qualitatively compared with the SW voltammograms of azobenzene recorded at a HMD electrode. The SW voltammetric response of  $1 \times 10^{-4}$  mol dm $^{-3}$  azobenzene solution recorded in 1 mol dm $^{-3}$  KNO $_3$  consists of a well developed, single SW peak located at  $E_p = -0.115$  V (Figure 11a). The voltammetric response appears as a result of a two-electron, chemically reversible reduction of azobenzene to hydrazobenzene, according to the scheme:

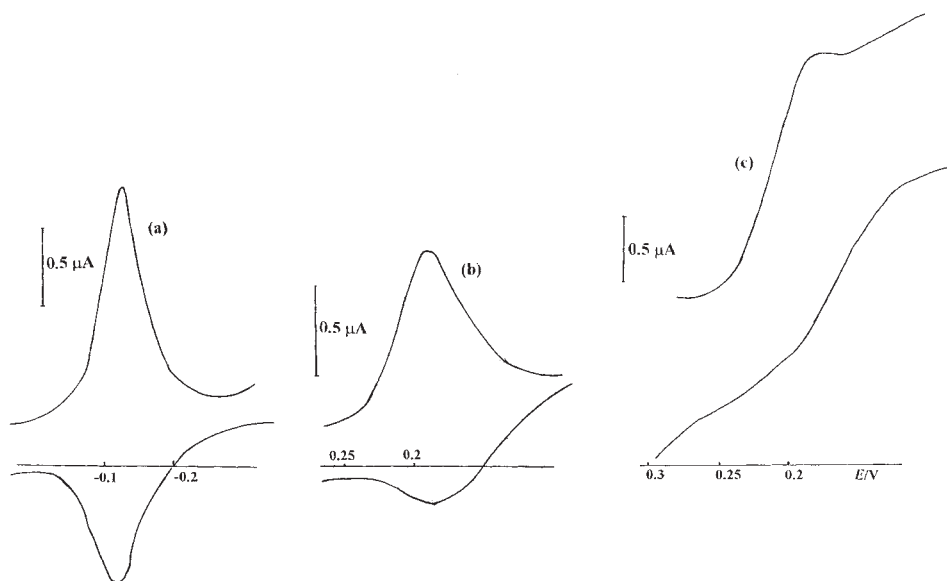


Figure 11. The cathodic and the anodic components of the SW voltammetric responses of  $1 \times 10^{-4}$  mol dm $^{-3}$  solution of azobenzene recorded in: 1 mol dm $^{-3}$  KNO $_3$  buffered with an acetate buffer to pH = 4.6 (a), 1 mol dm $^{-3}$  HNO $_3$  (b) and 2 mol dm $^{-3}$  HNO $_3$  (c). The other experimental conditions were:  $f = 50$  Hz,  $E_{\text{sw}} = 25$  mV,  $dE = 2$  mV,  $t_{\text{acc.}} = 30$  s (stirred solution), equilibrium time = 5 s,  $E_{\text{acc.}} = 0.3$  V.

The cathodic and the anodic branches of the SW response are symmetrically located with respect to the potential axis. Both branches bear the same peak potential, indicating that both azobenzene and hydrazobenzene are strongly immobilized at the mercury electrode surface.<sup>5,11-13,36,37</sup> Hydrazobenzene, being an electroreduction product of azobenzene, undergoes in

strong acidic medium intramolecular, chemically irreversible rearrangement to benzidine (4',4'-diaminobiphenyl). Benzidine, as the final product, is electroinactive. Therefore, in a strong acidic medium, the simple surface redox reaction of azobenzene turns into the surface EC mechanism.<sup>13</sup> The rate of the benzidine rearrangement is proportional to the concentration of protons in the supporting electrolyte. During the experimental work, the rate of the following chemical reaction can be readily controlled, matching the amount of the acid in the supporting electrolyte. Hence, the anodic branch of the SW response recorded in 1 mol dm<sup>-3</sup> HNO<sub>3</sub> is considerably diminished, as compared to the corresponding branch recorded in 1 mol dm<sup>-3</sup> KNO<sub>3</sub> (see Figure 11b). At the same time, all the components of the SW response are dislocated towards more positive potentials (Figure 11b). The rate of the benzidine rearrangement in 2 mol dm<sup>-3</sup> HNO<sub>3</sub> is sufficiently rapid to transform all of the electrochemically formed hydrazobenzene into the benzidine, and therefore the overall electrode reaction appears totally irreversible (Figure 11 c).

The net SW peak current of azobenzene depends sigmoidally on the logarithm of the HNO<sub>3</sub> concentration (Figure 12). This dependence corresponds to the theoretical dependency between the peak current and the logarithm of the chemical parameter  $\gamma$  (see Figure 2). The peak current shifts

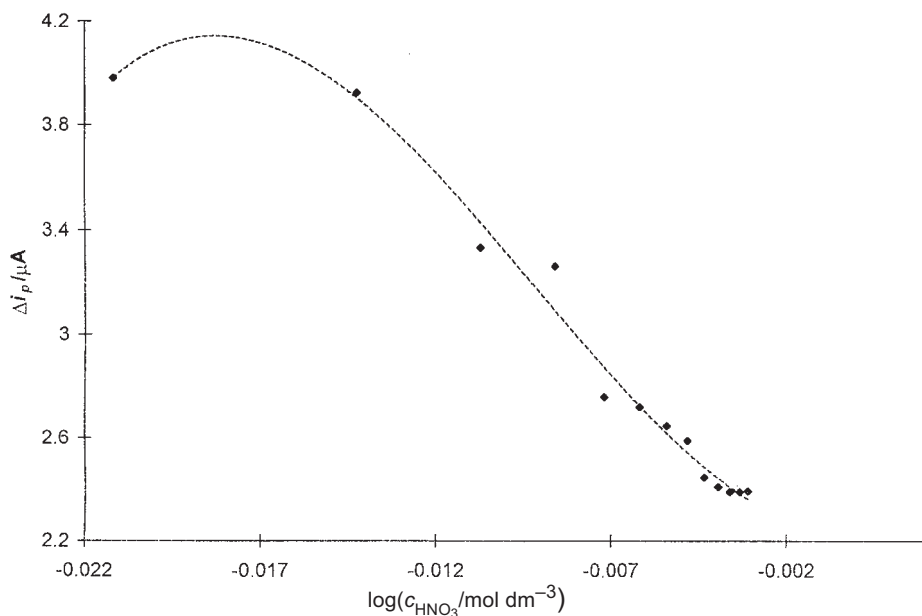


Figure 12. Dependence of the peak current of azobenzene and the logarithm of the nitric acid concentration. The frequency of the SW signal was  $f = 100$  Hz. All other conditions were the same as in Figure 11.

in positive direction with an increase of the acid concentration. If the concentration of the acid is  $\log(c_{\text{HNO}_3}) \geq -0.01$ , the electrode reaction appears irreversible. Under these experimental conditions, linear dependence was found between  $E_p$  and the logarithm of  $c(\text{HNO}_3)$ , which is consistent with the theoretical predictions.

When the SW amplitude was increased up to  $E_{\text{sw}} = 100$  mV, the SW response of azobenzene recorded in  $1 \text{ mol dm}^{-3} \text{ KNO}_3$  consisted of two peaks as a result of the splitting of the SW peak (Figure 13a). Adding a certain amount of nitric acid into the supporting electrolyte, the rate of the following chemical reaction increases, causing a decrease of the anodic peak, which appears at more negative potentials. If the concentration of the acid was equal

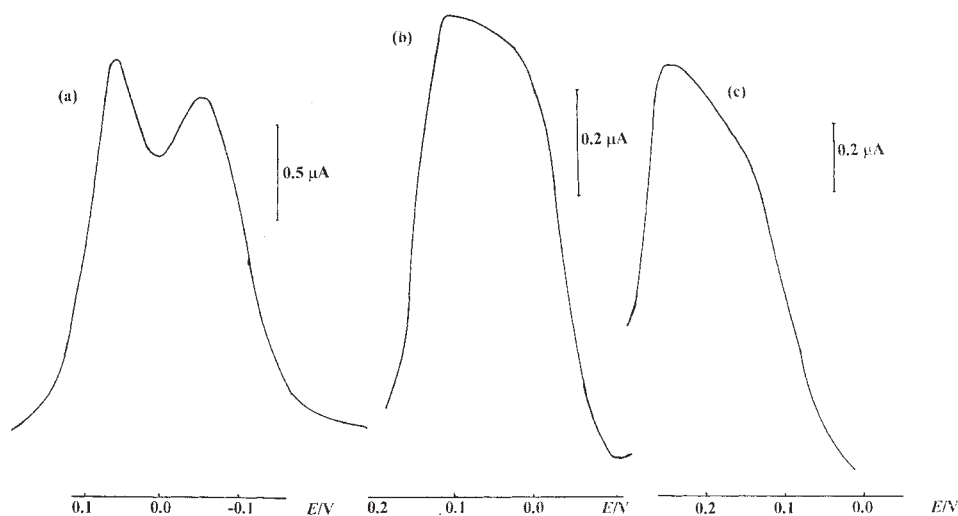


Figure 13. The effect of the concentration of the nitric acid on the splitting of the SW peak of azobenzene. Supporting electrolyte was:  $1 \text{ mol dm}^{-3} \text{ KNO}_3$  (a);  $0.04 \text{ mol dm}^{-3} \text{ HNO}_3$  (b) and  $0.08 \text{ mol dm}^{-3} \text{ HNO}_3$  (c). The frequency was  $f = 30$  Hz and the amplitude  $E_{\text{sw}} = 100$  mV. Other conditions were as in Figure 11.

to or higher than  $0.04 \text{ mol dm}^{-3}$ , the splitting of the peak vanished and only the cathodic peak was observed (Figures 13b, c). These results are in fairly good agreement with the theory and they confirmed unequivocally that the redox reaction of azobenzene in an acidic medium belongs to the reversible surface EC electrode mechanism, which is in agreement with the literature data.<sup>13</sup>

If the experiment was carried out at a constant acid concentration, the particular value of the chemical parameter  $\gamma$ , for the electrode reaction of

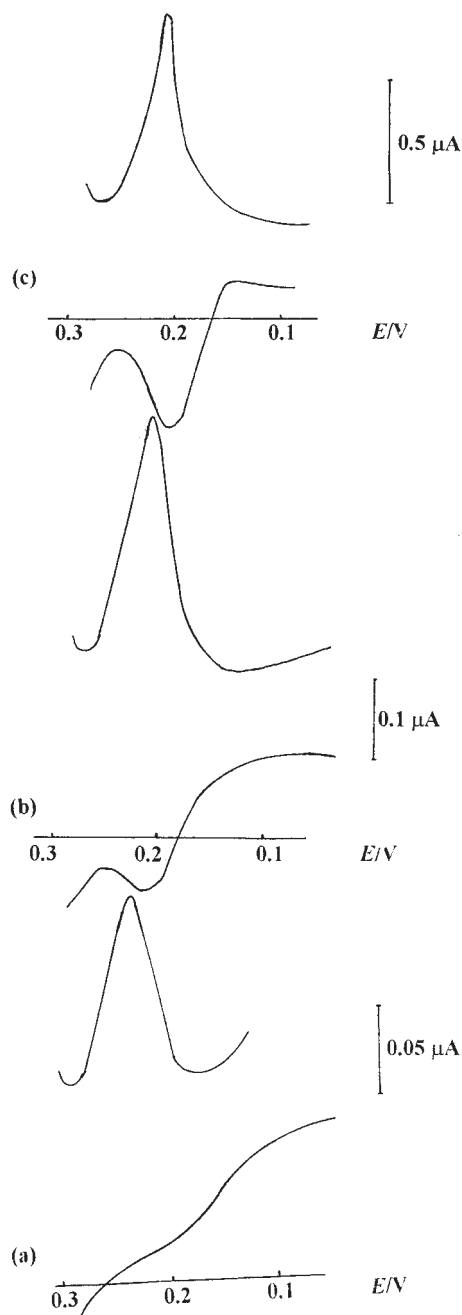


Figure 14. The effect of the frequency on the cathodic and anodic components of the SW response of azobenzene recorded in  $1 \text{ mol dm}^{-3} \text{ HNO}_3$ . The frequency of the signal was  $f = 10$  (a); 50 (b) and 200 Hz (c). All other conditions were as in Figure 11.

azobenzene, could be changed by the varying the signal frequency. Figure 14 shows how the frequency of the signal changes the apparent reversibility of the electrode process due to its influence on the chemical parameter  $\gamma$ . At the lowest frequency  $f = 10$  Hz, the chemical parameter  $\gamma$  bears the highest value and, consequently, the electrode reaction is totally irreversible (Figure 14a). Enhancement of the frequency resulted in an increase of the anodic branch of the SW response because the chemical parameter  $\gamma$  was diminished (Figure 14b). When the frequency is increased up to  $f = 200$  Hz, the influence of the chemical parameter is negligible and the redox reaction of azobenzene appears reversible (Figure 14c). Further increase of the frequency can affect the reversibility of the redox reaction only through the kinetic parameter  $\omega = k_s/f$ . If the frequency of the signal is increased above 200 Hz, the redox reaction of azobenzene gradually becomes quasireversible. Due to the effect of the quasireversible maximum, the ratio  $\Delta i_p/f$  (this ratio corresponds to the dimensionless peak current) commences to increase, reaching a maximum value for  $f = 600$  Hz (Figure 15). Hence, these results demonstrate the existence of the quasireversible maximum of the surface EC mechanism, which was theoretically predicted. All the above presented results confirm the validity of the theoretical models for SW voltammetry of the EC mechanism coupled with adsorption phenomena of the electroactive species.

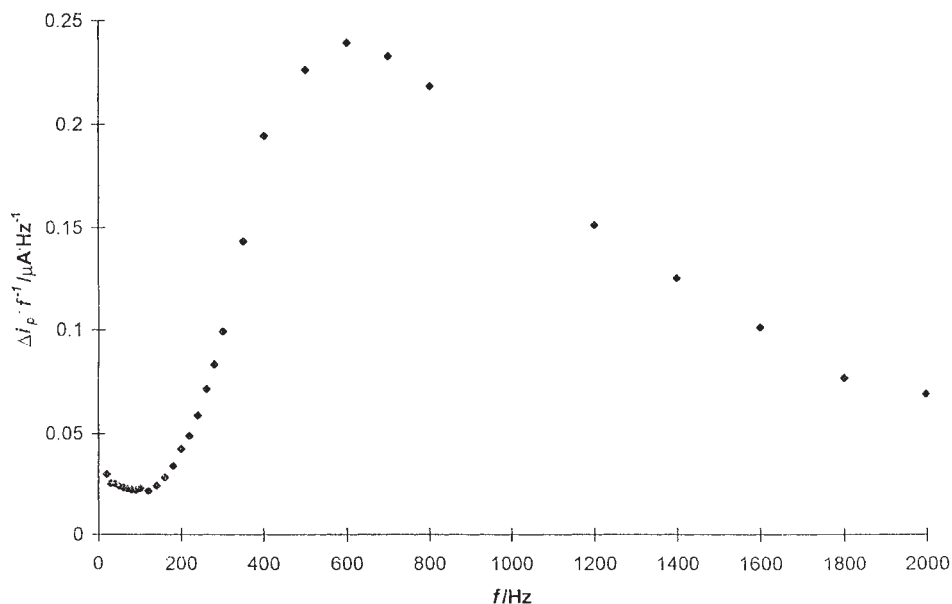


Figure 15. The quasireversible maximum of azobenzene recorded in  $1 \text{ mol dm}^{-3} \text{ HNO}_3$ . All other conditions were as in Figure 11.

## REFERENCES

1. W. M. Schwarz and I. Shain, *J. Phys. Chem.* **69** (1965) 30–40.
2. W. M. Schwarz and I. Shain, *J. Phys. Chem.* **70** (1966) 845–852.
3. R. H. Wopschall and I. Shain, *Anal. Chem.* **39** (1967) 1535–1542.
4. T. H. Ridgway, R. P. Van Duyne, and C. N. Reilley, *J. Electroanal. Chem.* **34** (1972) 267–282.
5. R. P. Van Duyne, T. H. Ridgway, and C. N. Reilley, *J. Electroanal. Chem.* **34** (1972) 283–295.
6. E. Laviron, *J. Electroanal. Chem.* **35** (1972) 333–342.
7. E. Laviron, *J. Electroanal. Chem.* **42** (1973) 415–422.
8. J. J. O'Dea, J. G. Osteryoung, and R. A. Osteryoung, *Anal. Chem.* **53** (1981) 695–701.
9. L. Sin-rhu and F. Qiang-sheng, *Anal. Chem.* **54** (1982) 1362–1367.
10. M. Kim, *Anal. Chem.* **59** (1987) 2136–2144.
11. M. Lovrić, Š. Komorsky-Lovrić, and M. Branica, *Croat. Chem. Acta* **66** (1993) 279–288.
12. Š. Komorsky-Lovrić and M. Lovrić, *Electroanalysis* **6** (1994) 651–656.
13. E. Laviron, *J. Electroanal. Chem.* **391** (1995) 187–197.
14. D. M. H. Kern, *J. Am. Chem. Soc.* **76** (1953) 1011–1015.
15. A. C. Testa and W. H. Reinmuth, *Anal. Chem.* **33** (1961) 1320–1324.
16. K. B. Wilberg and T. P. Lewis, *J. Am. Chem. Soc.* **92** (1970) 7154–7160.
17. R. S. Nicholson and I. Shain, *Anal. Chem.* **36** (1964), 706–723.
18. H. Y. Cheng and R. L. McCreery, *Anal. Chem.* **50** (1978) 645–647.
19. M. Mohammad, *Anal. Chem.* **49** (1977) 60–61.
20. J. G. Osteryoung and R. A. Osteryoung, *Anal. Chem.* **57** (1985) 101A–102A.
21. M. Lovrić, Š. Komorsky-Lovrić, and R. W. Murray, *Electrochim. Acta*, **33** (1988) 739–744.
22. M. Lovrić and Š. Komorsky-Lovrić, *J. Electroanal. Chem.* **248** (1988) 239–253.
23. M. Lovrić, Š. Komorsky-Lovrić, and A. M. Bond, *J. Electroanal. Chem.* **319** (1991) 1–18.
24. J. J. O'Dea, A. Ribes, and J. G. Osteryoung, *J. Electroanal. Chem.* **345** (1993) 287–301.
25. Š. Komorsky-Lovrić and M. Lovrić, *J. Electroanal. Chem.* **384** (1995) 115–122.
26. M. Lovrić and M. Mlakar, *Electroanalysis* **7** (1995) 1121–1125.
27. Š. Komorsky-Lovrić and M. Lovrić, *Anal. Chim. Acta* **305** (1995) 248–255.
28. J. J. O'Dea and J. G. Osteryoung, *Anal. Chem.* **69** (1997) 650–658.
29. V. Mirčeski and M. Lovrić, *Electroanalysis* **9** (1997) 1283–1287.
30. J. J. O'Dea and J. G. Osteryoung, *Anal. Chem.* **65** (1993) 3090.
31. H. J. Shine, *Aromatic Rearrangements*, Elsevier, Amsterdam, 1967, pp. 124–179.
32. L. Chuang and P. J. Elving, *Anal. Chem.* **37** (1965) 1506–1528.
33. P. N. Gupta and A. Raina, *J. Indian Chem. Soc.* **62** (1985) 363–366; **65** (1988) 495–497.
34. G. S. Hammond and H. J. Shine, *J. Am. Chem. Soc.* **72** (1950) 220–221.
35. D. A. Blackadder and C. Hinshelwood, *J. Chem. Soc.* (1957) 2898–2904.
36. J. Barek and R. Hrnčir, *Collect. Czechoslov. Chem. Commun.* **51** (1986) 25–33.
37. G. Pezzatini and R. Guidelli, *J. Chem. Soc., Faraday Trans. I* (1973) 794–805.
38. R. S. Nicholson and M. L. Olmstead, in J. S. Mattson, H. B. Mark, and H. C. MacDonald (Eds.), *Electrochemistry: Calculations, Simulation and Instrumentation*, Vol. 2. Marcel Dekker, New York, 1972, pp. 120–137.

**SAŽETAK****Utjecaj adsorpcije na odzive EC mehanizma mjerene voltammetrijom s pravokutnim valovima potencijala**

*Valentin Mirčeski i Milivoj Lovrić*

Teorijski je istražen utjecaj adsorpcije reaktanta i produkata dvaju EC mehanizama na odzive izazvane voltammetrijom s pravokutnim valovima potencijala. Akronim EC označuje mehanizam u kojem je produkt redoks-reakcije reaktant uzastopne kemijske reakcije. Razvijeni su teorijski modeli EC mehanizama u kojima se ili samo reaktant ili i reaktant i produkt elektrodne reakcije adsorbiraju na površinu radne elektrode. Razmatran je utjecaj kinetike redoks-reakcije na odzive oba EC mehanizma. Analizirana je ovisnost svojstava voltammetrijskih odziva o parametrima pobude i kinetičkim parametrima elektrodne reakcije. Teorijski rezultati kvalitativno su provjereni usporedbom s voltamogramima azobenzena u kiselom mediju.